THE ASTROPHYSICAL JOURNAL, 399:L79–L82, 1992 November 1

METHANOL ICE IN THE PROTOSTAR GL 2136

C. J. SKINNER[1]
Institute of Geophysics and Planetary Physics, L-413, Lawrence Livermore National Laboratory, P.O. Box 808, Livermore, CA 94551-9900
A. G. G. M. TIELENS
NASA-Ames Research Center, MS245-6, Moffett Field, CA 94035
AND
M. J. BARLOW AND K. JUSTTANONT[2]
Department of Physics & Astronomy, University College London, Gower Street, London WC1E 6BT, England, UK
Received 1992 June 26; accepted 1992 August 19

ABSTRACT

We present ground-based spectra in the 10 and 20 μm atmospheric windows of the deeply embedded protostar GL 2136. These reveal narrow absorption features at 9.7 and 8.9 μm, which we ascribe to the CO-stretch and CH_3 rock (respectively) of solid methanol in grain mantles. The peak position of the 9.7 μm band implies that methanol is an important ice mantle component (i.e., $CH_3OH/H_2O > 0.5$). However, the CH_3OH/H_2O abundance ratio derived from the observed column densities is only 0.1. This discrepancy suggests that the solid methanol and water ice are located in independent grain components. These independent components may reflect chemical differentiation during grain mantle formation and/or partial outgassing close to the protostar.

Subject headings: dust, extinction — ISM: abundances — ISM: individual (GL 2136) — ISM: molecules

1. INTRODUCTION

Icy grain mantles are an important component of interstellar dust inside dense molecular clouds (see Tielens 1989 for a review). Such icy grain mantles are formed by the accretion and reaction of gas phase species onto preexisting grain cores (Tielens & Hagen 1982; d'Hendecourt, Allamandola, & Greenberg 1985; Brown, Charnley, & Millar 1988). These icy grain mantles may lock up a considerable fraction of the condensible elements inside dense cloud cores. They may also form a source of gas phase molecules, particularly around newly formed stars (Walmsley 1989). Furthermore, UV processing of these icy mantles may lead to the formation of a complex organic residue. This organic grain mantle will be more refractory than the original ice mantle and could possibly exist even in the diffuse interstellar medium. Indeed, the observed presence of organic grains in the diffuse interstellar medium has been ascribed to this process (Butchart et al. 1985). Finally, it is often thought that interstellar icy grain mantles were the building blocks from which comets in our solar system were assembled (Greenberg 1982).

The infrared spectra of objects located within or behind molecular clouds commonly show absorption features due to molecules in these icy grain mantles (Willner et al. 1982; Lacy et al. 1984; Whittet et al. 1985, 1988; Tielens & Allamandola 1987a; Smith, Sellgren, & Tokunaga 1989). Besides H_2O and CO, CH_3OH is thought to be one of the dominant molecules in interstellar ice mantles. However, CH_3OH abundance estimates are quite controversial and range from 5% to 50% of that of H_2O (Tielens & Allamandola 1987a; Grim et al. 1991; Schutte, Tielens, & Sandford 1991). In general, abundance estimates based on the CH deformation mode at 6.85 μm indicate high CH_3OH/H_2O ratios, while those based on the CH stretching mode at 3.5 μm imply low ratios. Possibly, this discrepancy results from an incorrect assignment of the 6.85 μm band to methanol. Indeed, given the low spectral resolution, the 6.85 μm band could also be attributed to molecules other than CH_3OH (Grim et al. 1991). Alternatively, the discrepancy in the abundance estimates might reflect variations in the CH_3OH/H_2O ratio from source to source as well as within sources. Finally, the discrepancy might result from optical depth effects at the wavelengths of the different absorption features. In that scenario, the methanol column densities derived at 3.5 μm refer to material along the poles of the bipolar IR reflection nebulae associated with protostars (Pendleton, Tielens, & Sandford 1990). In contrast, the 6.85 μm column density pertains to disk material.

In an attempt to resolve these issues, we have searched for the strong CO stretching mode of methanol at 9.7 μm in the protostar, AFGL 2136. In § 2, we discuss the observational procedure. These results are reported in § 3 and compared to laboratory data in § 4. Section 4 also compares the methanol column densities derived from our observations with those from other regions of the spectrum. Finally the results are summarized in § 5.

2. OBSERVATIONS

We observed GL 2136 on the United Kingdom Infrared Telescope (UKIRT) with the common-user spectrometer CGS3. CGS3 has an array of 32 photoconducting Si:As detectors and has three gratings to allow coverage of the 20 μm atmospheric window and the 10 μm atmospheric window at two different spectral resolutions. All spectra were taken using a 5″ aperture, and sky spectra using a rotating sector chopper were used to aid in cancelling atmospheric features. The telescope secondary was chopped east-west at 7 Hz with a throw of 30″.

---

[1] Nuffield Radio Astronomy Laboratories, Jodrell Bank, England; and Laboratory for Experimental Astrophysics, Lawrence Livermore National Laboratory.

[2] Also NASA-Ames Research Center.

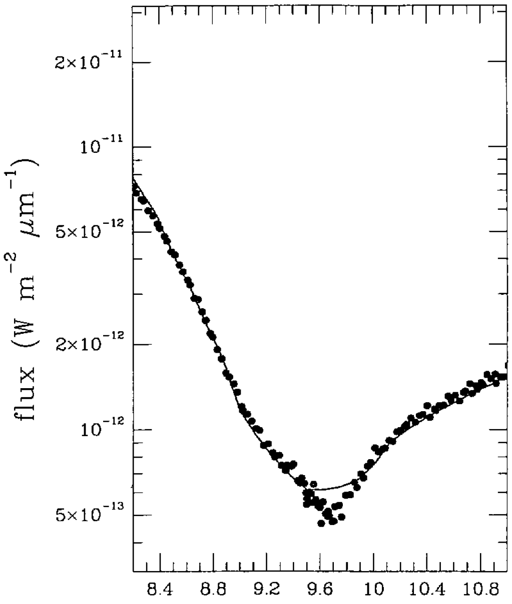

FIG. 1.—High-resolution CGS3 spectrum of GL 2136. The solid line shows the best model fit (see § 3).

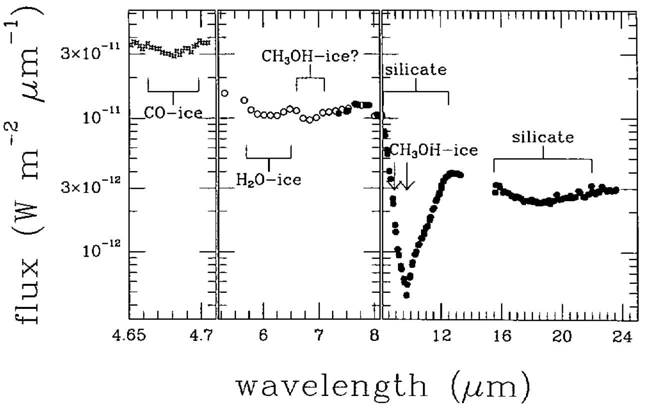

FIG. 2.—Montage of spectra of GL 2136. *Left panel:* solid CO absorption feature, taken from Tielens et al, 1991. *Center panel:* KAO low-resolution spectrum, from Tielens & Allamandola 1987a. *Right panel:* low-resolution CGS3 spectrum. The wavelengths of important features in the spectra are indicated.

Intermediate-resolution spectra ($\lambda/\Delta\lambda = 250$) centered at a wavelength of 9.7 μm and covering the 8.0–11.2 μm waveband were taken on 1991 May 23.6 U.T. Three different standard stars were observed: β Peg, β And, and α Lyr. The GL 2136 spectra were reduced using each of the three standards, since there is some concern that the spectra of M giants such as β Peg and β And may contain SiO absorption bands between 8 and 9 μm, while they are much brighter than α Lyr allowing higher signal-to-noise in the reduced spectra. In fact, we find there is no significant difference in the shape of spectra reduced with any of the three standards, and we will henceforth use the GL 2136 spectrum reduced using spectra of β Peg only. The reduced GL 2136 spectrum is shown in Figure 1.

Lower resolution spectra in the 10 μm atmospheric window ($\lambda/\Delta\lambda = 60$) and in the 20 μm atmospheric window ($\lambda/\Delta\lambda = 75$) were taken on 1991 May 24.6 U.T. These were again calibrated using spectra of β Peg, and the resulting spectra are shown in Figure 2. KAO spectra in the 5–8 μm region have been previously published (Tielens & Allamandola 1987a), and are included in Figure 2: these show absorptions due to water ice at 6.0 μm and the suggested methanol feature at 6.85 μm. Finally, a high-resolution spectrum showing the 4.675 μm solid CO absorption (Tielens et al. 1991) is also included in Figure 2.

3. ANALYSIS

A small triangular feature in absorption is evident in both low- and high-resolution spectra at a wavelength of ~9.7 μm. This is approximately the wavelength of the expected feature due to methanol ice. However, the situation is complicated by the superposition of the relatively weak ice absorption on the bottom of the very strong silicate dust absorption. Disentangling the two features is no mean feat, as the exact spectral profile of the silicate dust feature is known to vary from source to source (e.g., Tielens 1990).

In order to determine the profile of the suspected methanol ice absorption, we have used a χ-squared fitting program to fit a dust emissivity to the silicate feature in our high-resolution 8.0–11.1 μm observations. The program is due to Whitmore (1986) and fits emissivity data (in the form of mass absorption coefficients) to observed spectra by minimizing the value of χ-squared. A variety of emissivity data were available, including laboratory measurements of olivine and enstatite by Stephens & Russell (1979), and emissivity functions derived from observations of the Trapezium nebula in Orion and the M supergiant μ Cephei. A mixture of olivine and enstatite was found to give the best fit to the silicate feature in GL 2136 ($\chi^2 = 3.06$; if we ignore the 9.4–9.9 μm waveband, where the methanol ice absorption occurs, we get $\chi^2 = 1.07$); this was also found to give the best fit to 10 μm spectra of various red giants by Whitmore (1986). The fit thus determined is presented in Figure 1. No combination of silicate emissivity data could fit the suspected ice feature at 9.7 μm, corroborating our suspicion that this is not part of the silicate dust absorption.

The fitted silicate dust absorption feature was divided into the observed spectrum in order to determine the ice feature profile, which is presented in Figure 3. The error bars are simply those from the observed GL 2136 spectrum, and the 9.7 μm methanol ice feature is detected at a signal-to-noise ratio ~5. A second narrow feature is evident at a wavelength of ~8.9 μm at a similar signal-to-noise ratio. This corresponds to the weaker CH_3 rock of solid methanol presented by Schutte et al. (1991). The optical depth plot (Fig. 3) shows some slope at the short-wavelength end, which can be seen, by inspection of Figure 1, to be due to an imperfect cancellation of the silicate profile or continuum. Such imperfections cannot be invoked to explain the narrow absorption features seen in the plot, however. Identical results have been obtained using the above procedure with the GL 2136 spectra obtained using β And or α Lyr as standards, but with lower signal-to-noise ratio. Given a perfect fit to the GL 2136 silicate feature, the data either side of the ice features in Figure 3 should average zero. In reality, the fit of the silicate feature is not perfect, and some zero level adjustment should be made to the ice features in order to calculate the flux absorbed. However, the shape of the silicate feature is well reproduced by our fit, and thus the shape of the ice features should be correct. Finally, we have fitted silicate emissivity data due to Draine & Lee (1984) to the 9.7 and 18 μm silicate features in our low-resolution spectra, from which we derive optical depths of 2.3 and 0.7.

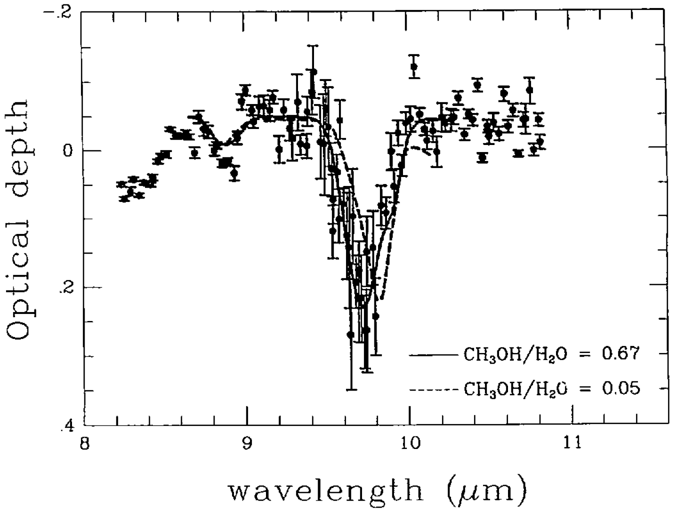

FIG. 3.—Optical depth of the features ascribed to solid methanol, with 1 σ errors. The solid line shows laboratory measurements of the absorption strength of a 2:1 mixture of methanol-ice:water-ice. The dashed line likewise shows laboratory measurements of the absorption strength of a 1:19 mixture of methanol-ice:water-ice.

4. DISCUSSION

Although we realize that substructure in the 10 μm feature might be intrinsic to the silicate material producing the absorption feature (e.g., crystalline Mg-rich olivines), we tentatively attribute the weak 9.7 and 8.9 μm bands to the CO stretch and CH_3 rock in methanol in interstellar grain mantles. There are several reasons for this. First, the observed bands compare very well in position and width with laboratory spectra of CH_3OH/H_2O mixtures with CH_3OH/H_2O ratios larger than 50% (Fig. 3; see below). Second, the CH stretching mode of CH_3OH at 3.5 μm has unambiguously been detected in several protostellar spectra (Grim et al. 1991; Allamandola et al. 1992). Analysis of these data shows that, after H_2O ice itself, methanol is the second most abundant grain mantle component. Since the C–O stretching mode at 9.8 μm is ~3 times stronger than the 3.5 μm methanol band, its presence might be expected. Third, AFGL 2136 and many other protostellar sources show a prominent 6.85 μm band, which has been assigned to the CH deformation mode in methanol (Tielens & Allamandola 1987a). Fourth, gas phase methanol is observed to be very abundant in warm regions around protostars (i.e., the compact ridge in the Orion BN/KL region) whose composition seem to be dominated by evaporation of icy grain mantles (Walmsley 1989). Finally, we emphasize that moderate-resolution ($\lambda/\Delta\lambda \sim 500$) spectroscopy in the 3.5 and 6.8 μm regions of the spectrum can unambiguously test for the presence of methanol in AFGL 2136 and the proposed identification of the 9.7 μm band. Laboratory spectra of mixtures of CH_3OH and H_2O show that the peak wavelength of the stronger C-O mode varies from 9.8 to 9.7 μm when the CH_3OH/H_2O ratio increases from ~0.2 to 0.5 (Schutte et al. 1991; see also their laboratory data reproduced in Fig. 3). The observed 9.7 μm feature in AFGL 2136 is best fitted by CH_3OH/H_2O mixtures with a ratio larger than 50%. Mixtures with CH_3OH concentrations less than 50% peak at too long a wavelength to explain the observed substructure in the silicate band. Thus, we conclude that methanol, if responsible for the weak 9.7 μm subpeak, has to be an abundant component of the icy grain mantles along the line of sight toward AFGL 2136. We determine equivalent widths of 0.0094 and 0.066 μm for the 8.9 and 9.7 μm bands, respectively (with estimated errors of 35% and 25%, respectively). Using the methanol band strengths presented by Schutte et al. (1991), which have an estimated uncertainty of 25%, these give us methanol column densities of $7.2(\pm 3.6) \times 10^{17}$ and $3.9(\pm 2.3) \times 10^{17}$ cm^{-2} from the 8.9 and 9.7 μm bands, respectively. These determinations are in reasonable agreement, and the mean is 5.5×10^{17} cm^{-2}. There is a hint of the 3.5 μm CH stretching mode in an unpublished 3 μm spectrum of GL 2136 (T. R. Geballe, private communication). This translates into a methanol column density of $3(\pm 2) \times 10^{17}$ cm^{-2}, slightly smaller than the values derived from the 8.9 and 9.7 μm bands. These methanol ice column densities are an order of magnitude less than the H_2O ice column density observed toward this source (Table 1), and the CH_3OH/H_2O ratio of 0.1 derived from these column densities is considerably less than the ratio required to fit the observed peak position.

One possible explanation for this discrepancy is that the 9.7 μm band could arise from (almost) pure methanol grain mantles which, however, cover only a minor fraction of the grains along the line of sight. In this interpretation, most of the grains would be covered by H_2O ice mantles without CH_3OH. Studies of the solid CO band have shown that, along many

TABLE 1

MOLECULAR ICE BANDS IN GL 2136

Species	Mode	ν (cm^{-1})	FWHM (cm^{-1})	λ (μm)	$\sigma_{\rm int}$ (cm^2 μm mol^{-1})	τ	N (cm^{-2})	X[a]
H_2O[b,c]	OH stretch	3254	240	3.073	1.9×10^{-19}	2.8	4.5×10^{18}	1.2×10^{-4}
CH_3OH[b,c]	CH stretch	2827	30	3.537	8.3×10^{-21}	0.06	3.0×10^{17}	7.8×10^{-6}
CO	CO stretch	2136	9	4.68	4.4×10^{-20}	0.2	1.1×10^{17}	2.9×10^{-6}
H_2O[d]	OH bend	1670	98	5.988	2.9×10^{-20}	0.4	5.7×10^{18}	1.5×10^{-4}
CH_3OH[b]	CH & OH deformation	1450	100	6.849	5.7×10^{-20}	0.4	3.1×10^{18}	8.1×10^{-5}
CH_3OH[b]	CH_3 rock	1128	15	8.865	1.3×10^{-20}	0.07	7.2×10^{17}	1.8×10^{-5}
CH_3OH[b]	CO stretch	1026	30	9.74	1.7×10^{-19}	0.2	3.9×10^{17}	1.0×10^{-5}
Silicate[e]	SiO stretch	1030	220	9.7	1.1×10^{-18}	2.3	2.0×10^{18}	5.2×10^{-5}

[a] Calculated from abundance relative to the 9.7 μm silicate feature using data from Tielens & Allamandola 1987b.

[b] Molecular data from Schutte et al. 1991.

[c] Optical depth from Geballe (private communication).

[d] All data from Tielens & Allamandola 1987a.

[e] Band strength from Tielens & Allamandola 1987b; optical depth from this work.

lines of sight (but not AFGL 2136), the solid CO is not mixed in with the solid H_2O (Tielens et al. 1991), lending some support for such a model. Such a differentiation of the grain mantles along the line of sight might reflect thermal gradients (i.e., outgassing) around the protostar or they might reflect variations in grain surface chemistry along the line of sight. These observations shed some further doubt upon the identification of the 6.85 μm band in GL 2136 with the CH deformation mode of CH_3OH. However, we note that GL 2136 is a very complex IR source (Kastner, Weintraub, & Aspin 1992), and the lines of sight at different wavelengths are not necessarily the same. In particular, scattering through the poles will be much more important at 3 μm than at 7 μm. Likewise in the depth of the silicate feature one may not penetrate the disk and protostellar envelope to the same depth as at 7 μm. Additionally, the beam sizes used to take the 3, 7 and 10 μm spectra are radically different. Thus, the 6.85 μm CH_3OH identification cannot be totally excluded, the more since CH_3OH and H_2O are independent ice mantle components and outgasing could lead to highly variable CH_3OH/H_2O abundance ratios close to the source.

Further spectroscopic studies may elucidate these questions.

5. CONCLUSIONS

We have presented spectra at low- and intermediate-resolution in the 10 and 20 μm atmospheric windows of the deeply embedded protostar GL 2136. Spectra at both resolutions show narrow absorption features at 9.7 and 8.9 μm, which we tentatively ascribe to solid methanol in grain mantles. The observed 9.7 μm band is best fitted by laboratory spectra with a high CH_3OH concentration (>0.5). However, the CH_3OH/H_2O abundance ratio derived from the observed column densities is much smaller (less than 0.1), suggesting that CH_3OH and H_2O are not well mixed along the line of sight.

C. J. S. acknowledges the financial support of the U.K. Science and Engineering Research Council for part of the duration of this work. This work was also supported in part (C. J. S.) under the auspices of the US Department of Energy by Lawrence Livermore National Laboratory under Contract No. W-7405-ENG-48. We are grateful to many members of the UKIRT staff for assistance, and to Dr. L. J. Allamandola, whose comments inspired the observations.

REFERENCES

Allamandola, L. J., Sandford, S. A., Tielens, A. G. G. M., & Herbst, T. 1992, ApJ, submitted
Brown, P. D., Charnley, S. B., & Millar, T. J. 1988, MNRAS, 231, 409
Butchart, I., McFadzean, A. D., Whittet, D. C. B., Geballe, T. R., & Greenberg, J. M. 1986, ApJ, 154, L5
d'Hendecourt, L. B., Allamandola, L. J., & Greenberg, J. M. 1985, A&A, 152, 130
Draine, B. T., & Lee, H. M. 1984, ApJ, 285, 89
Greenberg, J. M. 1982, in Comets, ed. L. J. Wilkening (Tucson: Univ. Arizona Press), 131
Grim, R. J. A., Baas, F., Geballe, T. R., Greenberg, J. M., & Schutte, W. 1991, A&A, 243, 473
Kastner, J. H., Weintraub, D. A., & Aspin, C. 1992, ApJ, 389, 357
Lacy, J. H., Baas, F., Allamandola, L. J., Persson, S. E., McGregor, P. J., Lonsdale, C. J., Geballe, T. R., & van de Bult, C. E. P. 1984, ApJ, 276, 533
Pendleton, Y., Tielens, A. G. G. M., & Werner, M. W. 1990, ApJ, 349, 107
Schutte, W., Tielens, A. G. G. M., & Sandford, S. A. 1991, ApJ, 382, 523
Smith, R. G., Sellgren, K., & Tokunaga, A. T. 1989, ApJ, 344, 413
Stephens, J. R., & Russell, R. W. 1979, ApJ, 228, 870
Tielens, A. G. G. M. 1989 in Interstellar Dust, ed. L. J. Allamandola & A. G. G. M. Tielens (Dordrecht: Kluwer), 239
Tielens, A. G. G. M. 1990 in From Miras to Planetary Nebulae: Which Path for Stellar Evolution? ed. O. Mennessier & A. Omont (Gif-sur Yvette: Editions Frontières), 186
Tielens, A. G. G. M., & Allamandola, L. J. 1987a, in Physical Processes in Interstellar Clouds, ed. G. E. Morfill & M. Scholer (Dordrecht: Riedel), 333
———. 1987b, in Interstellar Processes, ed. D. J. Hollenbach & H. A. Thronson (Dordrecht: Reidel), 397
Tielens, A. G. G. M., & Hagen, W. 1982, A&A, 114, 245
Tielens, A. G. G. M., Tokunaga, A. T., Geballe, T. R., & Baas, F. 1991, ApJ, 381, 181
Walmsley, C. 1989, in Interstellar Dust, ed. L. J. Allamandola & A. G. G. M. Tielens (Dordrecht: Kluwer), 263
Whitmore, B. 1986, Ph.D. thesis, University of London
Whittet, D. C. B., Bode, M. F., Longmore, A. J., Adamson, A. J., McFadzean, A. D., Aitken, D. K., & Roche, P. F. 1988, MNRAS, 233, 321
Whittet, D. C. B., Longmore, A. J., & McFadzean, A. D. 1985, MNRAS, 216, 45P
Willner, S. P., et al. 1982, ApJ, 253, 174